Rotation and Properties of Turbulence in W7-X

A. Krämer-Flecken[1], G. Fuchert[2], O. Grulke[2], M. Hirsch[2], D. Prisiazhniuk[3]
J. L. Velasco[4], T. Windisch[2] and the W7-X team

[1] *Institut für Energie- und Klimaforschung / Plasmaphysik, Forschungszentrum Jülich GmbH, D–52425 Jülich, Germany*

[2] *Max Planck Institut für Plasmaphysik, 17491 Greifswald, Germany*

[3] *Max Planck Institut für Plasmaphysik, 85748 Garching, Germany*

[4] *Laboratorio Nacional de Fusión, Madrid, Spain*

1 Introduction

Since December 2015 a Poloidal Correlation Reflectometer A. Krämer-Flecken et al. [1], Soldatov et al. [2], Prisiazhniuk et al. [3], Krämer-Flecken et al. [4] is in operation at W7-X Klinger et al. [5], Wolf, R. and the W7-X Team [6]. It belongs to a first set of diagnostics König et al. [7] which are installed at W7-X. The system is installed to measure the turbulence rotation as well as the turbulence properties in the plasma edge. The whole system shown in fig. 1 consists of 5 antenna mounted for O-mode polarization on a support structure and aiming to a common focal point at $R = 6\,\mathrm{m}, z = -0.1\,\mathrm{m}$. They are connected with $\approx 1.6\,\mathrm{m}$ Ka-band wave guides which end in a DN 150CF flange. The nearly straight and long in vessel wave guides are necessary to bridge the cryostat. The flange with the vacuum windows is locate on the AEA21 port which is positioned at $\phi = 72°$ and slightly below the mid plane.

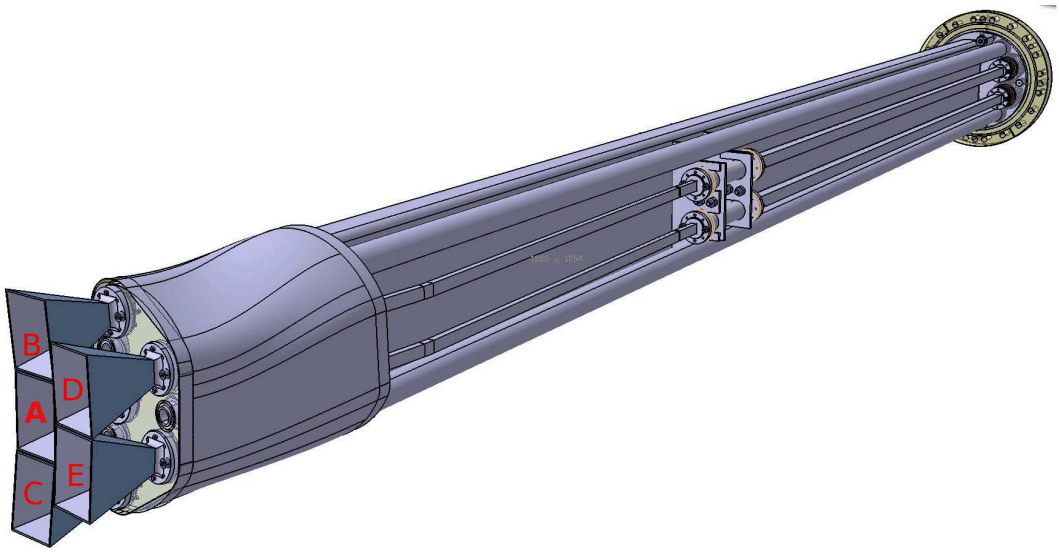

Figure 1: *Sketch of the plugin with the antenna array. The antenna are labeled with A for the launcher and B–E for the receiver.*

The reflectometer itself is operating in the frequency range 22 GHz to 40 GHz and consists

of a microwave synthesizer, generating two RF signals 30 MHz apart from each other, a frequency multiplier and low noise amplifiers. The reflected signal is mixed with the local oscillator frequency and afterwards detected by 4 IQ detectors sampled at a rate of 4 MHz. Due to the relatively low plasma electron density during the campaign OP1.1 the diagnostic was able to measure also in the plasma core and important observations regarding the transition to core electron root confinement (CERC) could be observed. Furthermore the transition from negative to positive rotation is observed in the plasma edge in the vicinity of the last closed flux surface (LCFS). First measurements of turbulence properties as decorrelation time and poloidal correlation length are performed as well.

2 Analysis methods

For the calculation of the turbulence velocity $v_\perp = \Delta s/\Delta t$ the viewing optics yielding Δs and the propagation or delay time Δt must be determined. In fig. 2 the poloidal separation for the combination EC and BC is shown. The effect of different plasma configuration

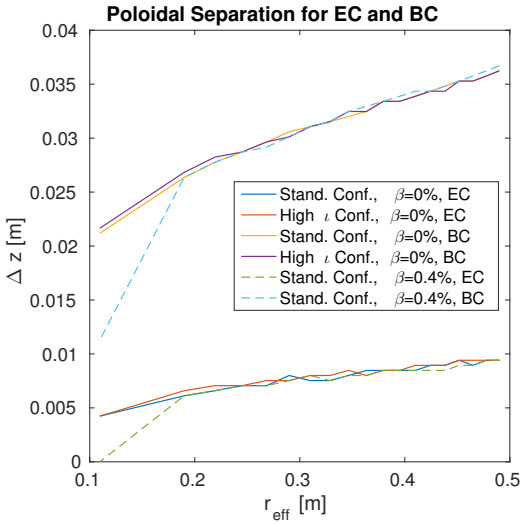

Figure 2: *Poloidal separation for combinations EC and BD for different VMEC configurations.*

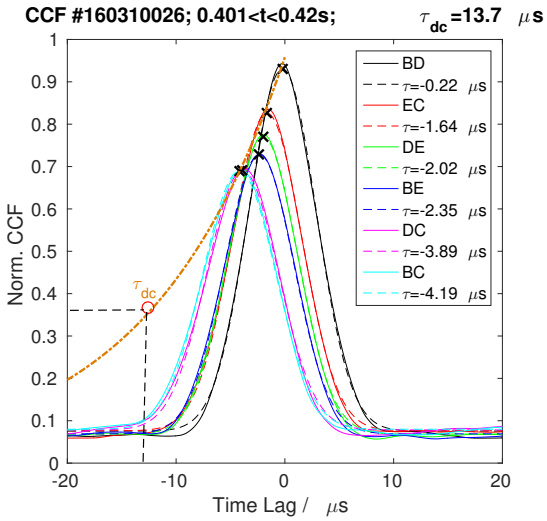

Figure 3: *CCF for all 6 antenna combinations. × mark the estimated Δt and the envelope is shown asdashed red curve from which the de-correlation time ist extracted.*

and plasma β on the poloidal separation up to the focal point is small ($\leq 8\,\%$) as shown in the figure. As a consequence the standard configuration is always used to calculated the poloidal separation. The delay time is calculated from the cross correlation function (CCF) of different combinations and is shown in fig. 3. The CCF can be described by a Gaussian modelPrisiazhnuik [8];

$$\rho(\Delta s, \tau) = \rho_0 exp\left(-\frac{(\Delta s - v_\perp \tau)^2}{l_{eff}^2} - \frac{\tau^2}{\tau_{dc}^2}\right) \tag{1}$$

where τ denotes the time lag, τ_{dc} the decorrelation time, l_{eff} the effective correlation length and Δs the separation between two receiving antenna with respect to the the direction of $B_\perp$. For a simplified calculation, only aiming in the exact determination of the delay time the equation

$$\rho(\Delta t, \tau) = A(\Delta t) exp\left(\frac{-(\tau - \Delta t)^2}{\sigma^2}\right) \tag{2}$$

is used. In this equation σ denotes the half width at half maximum and A denotes the amplitude of the CCF. The CCF of the six antenna combinations are used to calculate the envelope $h(\tau)$ of the CCF. The $1/e$ level of of $h(\tau)$ defines the decorrelation time of the turbulence. For all measurements, presented in this paper, the raw data used for the estimation of the CCF are filtered in a range of 5 kHz to 350 kHz when not otherwise mentioned. This frequency range is determined by a significant coherence and a good linearity of any two antenna combinations.
Further requirements for the calculation of $v_\perp$ is the knowledge of the reflection radius (r_c). For the estimation n_e-profiles from Thomson scattering Pasch et al. [9] are used. The 10 radial channels are described by a standard density profile of the form:

$$n_e(r_{eff}) = n_0 \left(1 - \left(\frac{r_{eff}}{a}\right)^p\right)^q \tag{3}$$

Taking further into account the distortions of the eddies as described in Prisiazhniuk et al. [3] $v_\perp$ can be expressed as:

$$v_\perp^* = v_\perp \left(1 - \left(\frac{< \tau_a >}{\tau_{dc}}\right)^2\right) \tag{4}$$

with $< \tau_a >$ denoting the mean autocorrelation time of all combinations. For the further discussion the phase velocity of the turbulence with respect to the plasma $v_{E\times B}$ is neglected. This is justified to some extent by measurements in Prisiazhniuk et al. [3] where the phase velocity for the drift ballooning modes dominating the gradient region of the plasma is much less than theoretically expected. This assumption allows to calculate the plasma velocity as $v_{turb} = v_\perp = v_{E\times B}$ and the related radial electric field $E_r = v_\perp B$.

3 Measurement of $v_\perp$ and E_r

Measurements of $v_\perp$ are performed on a regular basis for every discharge. Profiles of the plasma velocities are constructed by (i) varying the reflectometer frequency from shot to shot while keeping the plasma parameters constant or by (ii) hopping frequency operation with a step duration from 10 ms to 50 ms. In the vicinity of the plasma edge both

measurements show the change of sign in the plasma velocity. According to earlier investigations Nold et al. [10] this happens in the vicinity of the LCFS. In fig. 4 this transition is observed. In fig. 4a the contour lines of the plasma density are shown. The dashed line denotes r_c and the crosses denote the reflectometer position during the jumps from (i) 40 GHz to 22 GHz and back again from to 24 GHz 28 GHz. In fig. 4b the corresponding velocities are shown as function of r_{eff}. The jump in frequency from position 1 to 2 corresponds to a jump in r_{eff} of nearly 0.1 m. For position 3 the measurement is still outside the LCFS. However, at position 4,5 the velocity direction is again in electron drift direction. From positions 3 and 4 the radius of the LCFS is estimated to ≈ 0.47 m which is close to $r_{LCFS} = 0.49$ m as calculated from VMEC. In fig. 5a,b the transition across the LCFS is shown in more detail in a discharge with constant reflectometer frequency. Here,

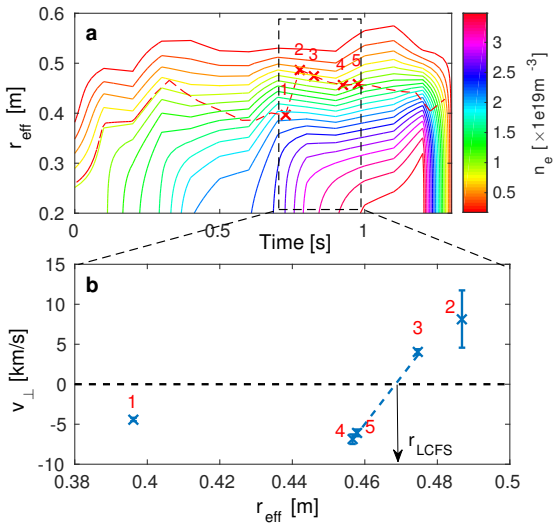

Figure 4: *Estimation of the LCFS for 160303.008. (**a**) Electron density contour with dashed r_c. Measurements are labeled by numbers. (**b**) $v_\perp$ in the transition region.*

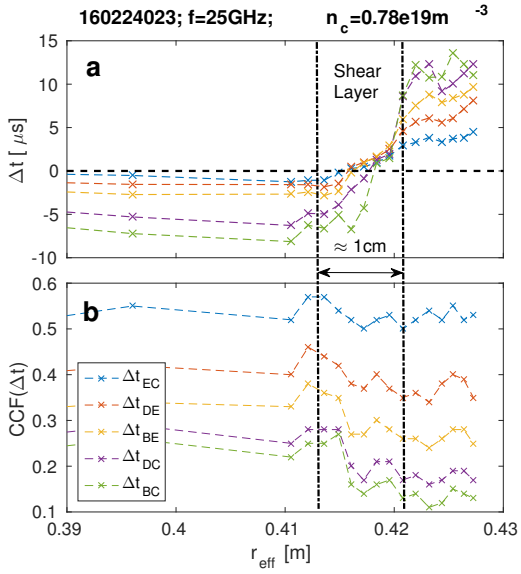

Figure 5: *(**a**) Delay times and (**b**) $CCF(\Delta t)$ estimated in the vicinity of the LCFS as function of r_{eff}.*

the electron density is slightly increasing and r_c is moving outward with $0.06\,\mathrm{m\,s^{-1}}$. The CCF for all combinations is calculated every 20 ms during the whole discharge. It is of interest that the transition to positive Δt values is observed at smaller radii as well as for small poloidal separation and therefore earlier than for combinations with larger poloidal separation. It could be evidence for the generation of eddies in shear layer with propagation in ion drift direction and whereas still larger eddies exist propagating in electron drift direction. However, the latter decrease very rapidly as can be seen in the reduction of the CCF values. Such kind of experiments could yield information on the mechanism in the shear layer and are planned for the next campaign.

Another interesting observation is the generation of high frequency modes in the coherence spectrum. In fig. 6 in the range 1.0 s to 1.1 s a sudden strong increase in the coherence level for the frequency range 170 kHz to 240 kHz is observed. This goes along with a reduction of the central coherence which also shrinks in its width. During this time the density profile show that the reflectometer cut-off position is still located in the plasma and $r_c = 0.34\,\mathrm{m}$ is found. This is in agreement with the increase of the cross phase slope for combinations with increasing poloidal separation. Furthermore it can bee seen from fig. 7 that the slope for the high frequency structure is positive, whereas the slope for the low frequency part is still negative. From the slope of the cross phase, $v_\perp$ can be calculated and the estimated wave number $k_\perp = 2\pi f / v_\perp$ is $2.5\,\mathrm{cm}^{-1} \leq k_\perp \leq 3.2\,\mathrm{cm}^{-1}$. Possible explanations for the observations are (i) Alfven waves where the fast particles must be generated by ECRH Windisch et al. [11] and (ii) ITG-modes which should be expected in the plasma core. To solve the origin of the high frequency structure more dedicated experiments should be performed in the next campaign.

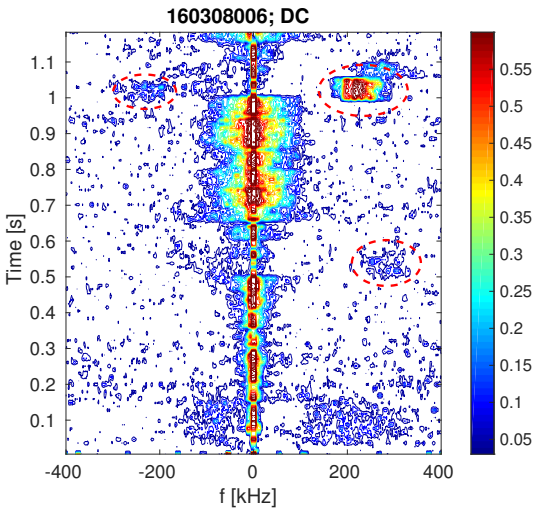

Figure 6: *Color coded coherence which shows the high frequency structure at* $t = 1.0\,\mathrm{s}$ *and* $170\,\mathrm{kHz} \leq f \leq 240\,\mathrm{kHz}$.

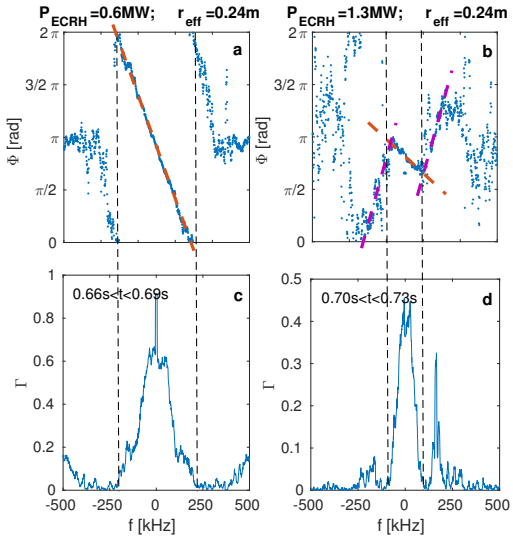

Figure 7: *Crossphase* ***a,b*** *and coherence* ***c,d*** *for two successive time intervals which demonstrate the dependence of the high frequency structure on* P_{ECRH}. *Note the different slopes in* ***b*** *for the low and high frequency.*

4 CERC plasmas

One of the major results in the plasma core was the observation of Core Electron Root Confinement (CERC). CERC plasmas are characterized by steep electron temperature profiles which are achieved by strong on axis ECRH heating. Furthermore a relative

low electron density supports the transition to the CERC regime. With a central density $1.5 \times 10^{19}\,\mathrm{m}^{-3} \leq n_e \leq 1.8 \times 10^{19}\,\mathrm{m}^{-3}$ the PCR system is able to measure $v_\perp$ and E_r in the plasma core. A draw back in this measurements is the flat n_e-profile which is responsible for a radial resolution of $\approx 0.04\,\mathrm{m}$ for O-mode polarization according to:

$$\Delta r_c = \frac{1.6 L_n}{([\omega_p/c] L_n)^{2/3}} \tag{5}$$

where L_n denotes the density scale length, ω_p the plasma frequency and c the speed of light. For the discharge *160309.010* the PCR was in hopping operation and $v_\perp$ (fig. 8a) and E_r (fig. 8b) profiles for the three different heating scenarios could be calculated. For the case with $P_{ECRH} = 0.6\,\mathrm{MW}$ a transition to the CERC regime at $r_{eff} = 0.2\,\mathrm{m}$ is observed. In addition a tendency for the other cases towards an increase of $v_\perp$ and E_r in the direction of positive values is observed. For the discharge *160310034* and the time interval $0.82\,\mathrm{s} \leq t \leq 1.2\,\mathrm{s}$ the PCR system scanned a frequency range 22 GHz to 40 GHz. The analysis of the flux surface averaged E_r from the PCR system is shown in fig. 9 and compared with neoclassical calculations using the direct kinetic equation solver (DKES). It demonstrates the good agreement of the DKES simulations with the measurements of the PCR system. Filtering of the PCR data $150\,\mathrm{kHz} \leq f \leq 350\,\mathrm{kHz}$ and calculating E_r shows also the transition to positive E_r in the center and at the same r_{eff} where it is expected from the DKES calculations.

5 Turbulence properties

This section describes results from the first analysis of turbulence properties at W7-X. The conception of turbulence based on the existence of small eddies which move mainly along a flux surface and have a certain life time and extension in all 3 dimensions. With the PCR diagnostic the measurement of the decorrelation time, τ_{dc}, (see section 2) and the effective poloidal correlation length, l_{eff}, is possible. The latter is calculate from the absolute value of $v_\perp$ and the auto correlation time (τ_a) as

$$l_{eff} = |v_\perp| \cdot \tau_a; \quad l_{eff} = \sqrt{l_\perp^2 + l_{sys}^2} \tag{6}$$

where $l_\perp$ is the real poloidal correlation length and l_{sys} the contribution from the detection volume size. This approximation is valid as long as $\tau_a < \tau_{dc}$. To quantify the latter is difficult and needs simulations of the reflection process itself.
Decorrelation time and effective correlation length are calculated for a series of discharges where the PCR system operates at fixed frequency during each discharge and the frequency was varied on a shot to shot basis. The results are summarized in figs. 10 and 11. A

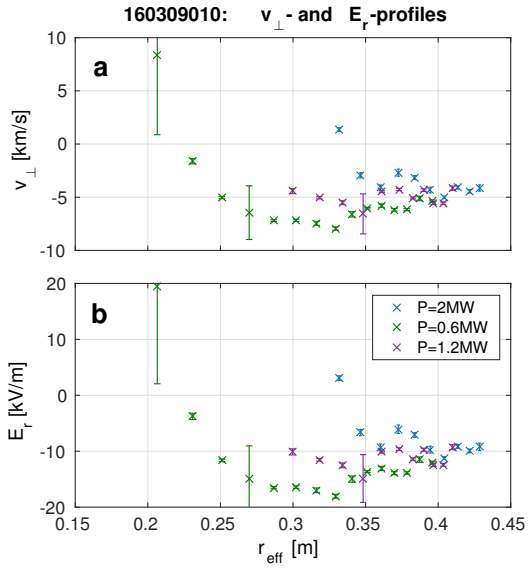

Figure 8: *(**a**) Calculated $v_\perp$ profiles for three different heating scenarions and (**b**) associated E_r profiles. Both $v_\perp$ and E_r profiles show the transition to the CERC regime in the plasma core.*

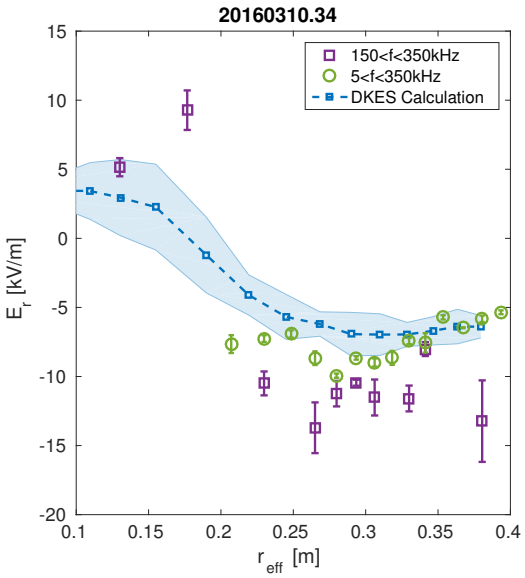

Figure 9: *Comparison of DKES from neoclassical calculation with the experimental data showing the good agreement between them. With the restriction to high frequencies the transition to CERC regime becomes visible.*

decrease of τ_{dc} towards the plasma edge is observed from values close to 15 µs in the core to 5 µs at the LCFS. In this region $v_\perp$ is constant. In the shear region at the LCFS τ_{dc} shows a large scatter which is presumable an effect generated by the trim coil of W7-X which were in scanning operation for those discharges. Regarding the estimation of l_{eff} it is found to be constant with a mean value of $< l_{eff} >= 26$ mm in the region with constant $v_\perp$. In the shear region a tendency towards an increased l_{eff} is observed. A scaling with ρ_s as reported from AUG experiments Prisiazhnuik [8] could not be confirmed. However, also in this case the effect of the trim coils on the plasma turbulence at the LCFS is not clear.

6 Summary and outlook

The commissioning of the PCR system at W7-X during the first operation campaign was successful. The system was stable during the whole campaign and could deliver information on the turbulence velocity. Neglecting any effects of an additional phase velocity the measured turbulence velocity is taken as a measure for the $v_{E\times B}$. The obtained velocity is negative and rotation profiles are nearly flat in the plasma core. At the plasma edge a shear layer was identified. The measurements show the capability of the PCR system to measure in the vicinity of the LCFS with good temporal and radial resolution.

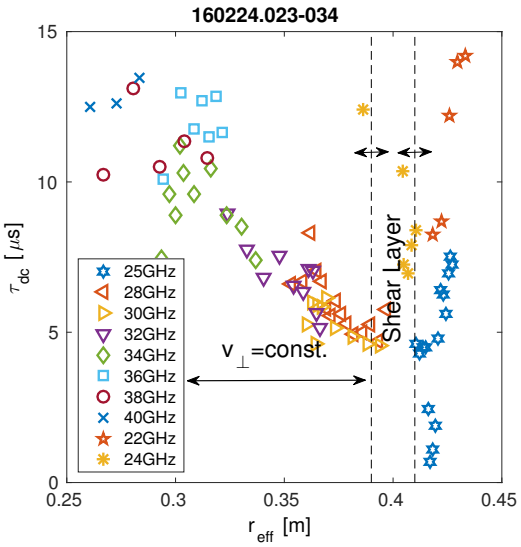

Figure 10: *Decorrelation time as function of r_{eff} for a series of identical plasmas. Decrease of τ_{dc} towarde the LCFS is observed.*

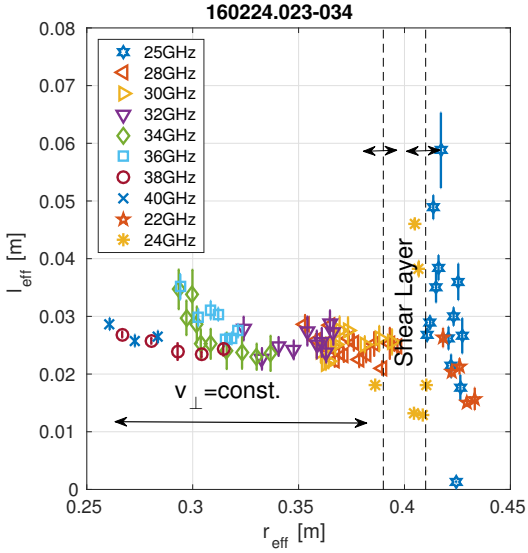

Figure 11: *Effective correlation length for the same series an in 10. A constant correlation length is observed.*

High frequency structures were found in the plasma core. However, the origin of these structures is not yet clear. Due to the relative low density the PCR system could measure deep in the core where a transition to CERC regime is expected. For several plasmas such a transition was observed. The comparison with NC calculations is in good agreement.
Also first investigations of turbulence decorrelation time and effective correlation length are performed. A decrease of the τ_{dc} towards the plasma edge and constant l_{eff} are observed.
For the next campaign the existing PCR diagnostic will be upgraded by another microwave synthesizer which will allow the measurement of radial correlations. It is intended to analyse than the radial correlation length which is an important quantity for the plasma transport. In addition to the PCR upgrade two other Doppler reflectometers will be installed in the same port as well as the launcher for the Alkali beam for the BES diagnostic. This suite of turbulence diagnostic at the same toroidal location will allow (i) cross comparison of physical quantities as $v_\perp$ and E_r and (ii) cross correlation analysis of different diagnostics which will of value for the reliability of the diagnostic and a deeper understanding of turbulence and transport in plasmas.

Acknowledgement

This work has been carried out within the framework of the EUROfusion Consortium and has received funding from the Euratom research and training programme 2014-2018 under grant agreement No 633053. The views and opinions expressed herein do not necessarily

reflect those of the European Commission.
This work was also performed in the framework of the Helmholtz Virtual Institute on Plasma Dynamical Processes and Turbulence Studies using Advanced Microwave Diagnostics.

References

[1] A. Krämer-Flecken, S. Soldatov, B. Vowinkel, and P. Müller. *Rev. Sci. Instrum.*, 81:113502, 2010. doi: http://dx.doi.org/10.1063/1.3497305. URL http://aip.scitation.org/doi/pdf/10.1063/1.3497305.

[2] S. Soldatov, A. Krämer-Flecken, and O. Zorenko. *Rev. Sci. Instrum.*, 82:033513, 2011. doi: http://dx.doi.org/10.1063/1.3567779. URL http://aip.scitation.org/doi/pdf/10.1063/1.3567779.

[3] D Prisiazhniuk, A Krämer-Flecken, G D Conway, T Happel, A Lebschy, P Manz, V Nikolaeva, U Stroth, and the ASDEX Upgrade Team. *Plasma Physics and Controlled Fusion*, 59(2):025013, 2017. doi: http://dx.doi.org/10.1088/1361-6587/59/2/025013. URL http://stacks.iop.org/0741-3335/59/i=2/a=025013.

[4] A. Krämer-Flecken, T. Windisch, W. Behr, G. Czymek, P. Drews, G. Fuchert, J. Geiger, O. Grulke, M. Hirsch, M. Knaup, Y. Liang, O. Neubauer, E. Pasch, J.L. Velasco, and The W7-X Team. *Nuclear Fusion*, 57 (6):066023, 2017. doi: https://doi.org/10.1088/1741-4326/aa66ae. URL http://stacks.iop.org/0029-5515/57/i=6/a=066023.

[5] T Klinger, A Alonso, S Bozhenkov, R Burhenn, A Dinklage, et al. *Plasma Physics and Controlled Fusion*, 59(1):014018, 2017. doi: http://dx.doi.org/10.1088/0741-3335/59/1/014018. URL http://stacks.iop.org/0741-3335/59/i=1/a=014018.

[6] Wolf, R. and the W7-X Team. First plasma operation in W7-X. pages CN–234/1–12. IAEA Fusion Energy Conference, Kyoto (Japan), 17 Oct 2016 - 22 Oct 2016, Oct 2017.

[7] R. König, J. Baldzuhn, W. Biel, C. Biedermann, H.S. Bosch, S. Bozhenkov, et al. *Journal of Instrumentation*, 10(10):P10002, 2015. doi: http://dx.doi.org/10.1088/1748-0221/10/10/P10002. URL http://stacks.iop.org/1748-0221/10/i=10/a=P10002.

[8] D. Prisiazhnuik. *Development and application of poloidal correlation reflectometry to study turbulent structures in the ASDEX Upgrade tokamak*. PhD thesis, Technical Univercity Munich, 2017.

[9] E. Pasch et al. pages P4.016/1–4. 43rd EPS Conference on Contr. Fusion and Plasma Phys., Leuven, Belgium, 4-8 July 2016, 2016. URL http://ocs.ciemat.es/EPS2016PAP/pdf/4.016.pdf.

[10] B Nold, G D Conway, T Happel, H W Mller, M Ramisch, V Rohde, U Stroth, and the ASDEX Upgrade Team. *Plasma Physics and Controlled Fusion*, 52 (6):065005, 2010. doi: http://dx.doi.org/10.1088/0741-3335/52/6/065005. URL http://stacks.iop.org/0741-3335/52/i=6/a=065005.

[11] T Windisch, A Krämer-Flecken, J.L. Velasco, et al. *Plasma Physics and Controlled Fusion*, 2017. doi: https://doi.org/10.1088/1361-6587/aa759b. URL http://iopscience.iop.org/10.1088/1361-6587/aa759b.